

# Sequence Detection Algorithms for Dynamic Spectrum Access Networks

Zhanwei Sun, and J. Nicholas Laneman, and Glenn J. Bradford  
Department of Electrical Engineering, University of Notre Dame  
E-mail: {zsun2, gbradfor, jnl}@nd.edu

**Abstract**—Spectrum sensing is a critical function for enabling dynamic spectrum access (DSA) in wireless networks that utilize cognitive radio. In DSA networks, unlicensed secondary users can gain access to a licensed spectrum band as long as they do not interfere with primary users. Spectrum sensing is subject to errors in the form of false alarms and missed detections. False alarms cause spectrum under-use by secondary users, and missed detections cause interference to primary users. Although existing research has demonstrated the utility of a Markov chain for modeling the spectrum access pattern of primary users over time, little effort has been directed toward spectrum sensing based upon such models. In this paper, we develop several soft-input sequence detection algorithms of Markov sources in noise for spectrum sensing in DSA networks. We assign different Bayesian cost factors for missed detections and false alarms, and we show that a suitably modified forward-backward sequence detection algorithm is optimal in minimizing the detection risk. Two advanced sequence detection algorithms, complete forward algorithm and complete forward partial backward algorithm are introduced and their performance are compared as well. Along the way, we observe new fundamental limitations on sensing performance that we term the *risk floor* and the *window length limitation* of energy detection and coherent detection that arise from their mismatch with the PU’s spectrum access pattern.

## I. INTRODUCTION

It is widely acknowledged that the traditional static allocation of wireless bandwidth by governmental regulators is spectrally inefficient due to spatial and temporal variation in utilization by licensed primary users (PUs). Dynamic spectrum access (DSA) is a promising approach for increasing spectrum efficiency by allowing unlicensed, secondary users (SUs) to opportunistically access the spectrum as long as they do not cause harmful interference to PUs. SUs employing DSA must accurately sense spectrum opportunities, often called spectrum holes, corresponding to gaps in PU transmissions. Spectrum sensing algorithms seek to balance the conflicting goals of minimizing interference to the PU while maximizing the rate of the SU. Performance of a sensing algorithm is typically characterized in terms of the probability of missed detection  $P_m$ , i.e., failing to sense the PU and thus causing interference, and the probability of false alarm  $P_f$ , i.e., falsely declaring that the PU is active and thus missing a spectrum opportunity. The inherent tradeoff between  $P_m$  and  $P_f$  for any detector leads to a tradeoff between these two aspects of system performance.

Classical physical (PHY) layer spectrum sensing approaches for a non-cooperating SU, such as coherent and energy detection [1], generally assume that any operating pair  $(P_f, P_m)$  is achievable at a given signal-to-noise ratio (SNR) as

long as a suitably long observation window is allowed. A notable exception arises if uncertainty exists in the statistics quantifying the channel, leading to the so-called SNR wall [2]. In practice, the observation length, and thus performance of the classical schemes, will be limited by the PU’s dwell time, which refers to the time duration of the PU staying in a particular state, whether ON or OFF. In fact, we will see that increasing the observation length beyond a certain point results in degraded performance. This limitation, which we call the *window length limitation*, occurs because the PU is observed in multiple states within a single sensing window.

Generally, the conditional probability that the spectrum is free in the next time instant is dependent on previous states of spectrum availability. Previous research has modeled the PU access pattern by a Markov chain. For example, the authors in [3] showed the Markov chain existence by real-time measurements collected in the paging band (928-948 MHz). Classical PHY-layer sensing approaches such as energy detection and coherent detection, however, fail to exploit this memory inherent in PU access patterns. In this paper, we develop several sequence detection algorithms derived from the well-known forward-backward algorithm and apply them to the problem of spectrum sensing where observations of the PU at the SU are assumed to follow a hidden Markov model. The proposed sequence detection algorithms not only incorporate the possible state change in the PU at any time instant, allowing sensing performance to continue to improve with sensing window length beyond the aforementioned limit, but also allow missed detections and false alarms to have different cost factors. Appropriate selection of the costs allows for operation at different  $(P_f, P_m)$  pairs. Additionally, we present a parameterization of the detector that allows a tradeoff between performance and sensing delay/complexity.

The remainder of the paper is organized as follows. In Section II, we summarize related work and compare these previous works to the results in this paper. In Section III, we introduce the hidden Markov model for the PU access pattern. In Section IV, we develop weighted sequence detection algorithms and show how they can be applied to the spectrum sensing problem. In Section V, we compare the proposed detection algorithms with energy and coherent detection and observe important limitations for the latter two. In Section VI, we provide numerical results demonstrating the improved performance of the proposed schemes as well as the limitations for energy and coherent detection. In Section VII, we conclude the paper.

## II. RELATED WORK

Spectrum sensing can be realized as a two-layer mechanism [4]. PHY-layer sensing focuses on efficiently detecting PU signals to identify opportunities by adapting the SU's transmission parameters. Several well-known PHY-layer detection methods such as energy detection, coherent detection, and feature detection have been extensively investigated [1], [2], [5], [6]. On the other hand, MAC-layer sensing determines when SUs have to sense which channels and for how long. Recently, significant effort has been devoted to the field of MAC-layer sensing and scheduling [4], [7], [8], [9].

In [7], the authors propose a joint channel sensing and transmission strategy in multichannel systems to maximize SU performance by intelligently deciding the sequence of channel probing/sensing and optimal action on each channel. In comparison, we do not employ two-stage sensing which requires MAC layer scheduling, but use the memory in the PU access pattern to make a final sensing decision.

In [4], the authors develop a sensing-period optimization mechanism and an optimal channel-sequencing algorithm, as well as an environment adaptive channel-usage pattern estimation method. We also discuss sensing-period optimization, however under the constraint of new limitations that we term the *risk floor* and the *window length limitation*. In contrast to the channel-sequencing algorithm that determined the order of multiple non-overlapping channels in which the SU should look for opportunities, our sequence detection algorithms simply focus on the fundamental case where only one channel is available to the SU. In [8], the authors introduce a more involved and efficient MAC-layer spectrum sensing scheme that takes advantage of both intrinsic and extrinsic knowledge about network states and environmental statistics. In comparison, our work only considers the PU's channel access pattern.

In [9], the authors formulate the spectrum sensing and transmission problems together as an optimal stopping algorithm that aims to maximize the average reward per unit time with a constraint on the collision cost. Specifically, a reward is received by a SU for each successful transmission and a penalty is received for a collision with the PU. In a similar way, we assign cost factors to tradeoff between PU protection and SU access performance. The authors assume the sensing time and cognitive transmission time are much smaller than an average PU busy or idle time. By comparison, we discuss the general case in which the SU's sensing and transmission time are comparable to a PU's busy or idle time.

Compared to these previous works, our main contributions are: 1) We introduce several sequence detection algorithms for spectrum sensing, which fully exploit the Markov memory modeling the PU's access pattern. 2) We assign cost factors and a risk function (both symbol-wise and sequence-wise) to make possible tradeoff between PU protection and SU access performance. 3) We derive new limitations for classical SU's PHY-layer sensing schemes.

## III. HIDDEN MARKOV MODEL

For simplicity of exposition, we assume there exists no multipath fading and all channel gains are constant. The PU's

behavior can take either slotted or unslotted structure. The SU is not synchronized with the PU, nor does the SU know anything about the slotted structure of PU. The PU's activity at any time instant (a sampling/symbol point at the SU) can be represented by a state, which can be either idle or busy. Let random variable  $S_t \in \{0, 1\}$  be the spectrum state at time  $t$ , where  $S_t = 0$  and  $S_t = 1$  correspond to the OFF state (PU inactive) and the ON state (PU active), respectively. Existing work has used Markov chain models for the channel state  $S_t$  [10] and the authors in [3] has validated its appropriateness based upon real-time measurements. In practical situations, higher-order Markov models may be used to better model other real world access patterns, but we focus on first-order models throughout this paper for which the conditional probability of the future states of the process, given the present state and the past states, depends only on the present state. Formally,

$$\begin{aligned} P(S_{t+1} = s_{t+1} | S_1 = s_1, \dots, S_t = s_t) \\ = P(S_{t+1} = s_{t+1} | S_t = s_t). \end{aligned} \quad (1)$$

Since only two states of the PU activities exist, the transition matrix of the Markov chain is

$$P = \begin{pmatrix} p_{00} & p_{01} \\ p_{10} & p_{11} \end{pmatrix}, \quad (2)$$

where  $p_{ij}$  is the probability of transition from state  $i$  to state  $j$  at any given time instant. Let the random variables  $L_0$  and  $L_1$  denote the dwell time of a PU's ON and OFF period, respectively. Because the transitions between ON and OFF periods of the PU are assumed to follow a first-order Markov process,  $L_0$  and  $L_1$  will be geometrically distributed with parameters  $p_{01}$  and  $p_{10}$ , respectively, i.e.,  $\mathbf{E}[L_0] = 1/p_{01}$  and  $\mathbf{E}[L_1] = 1/p_{10}$ , where  $\mathbf{E}[\cdot]$  is the expectation of a random variable. To fully specify the Markov chain we also need to know the initial distribution of the states, i.e., the probabilities that the sequence starts in state  $s_i$ ,

$$\Pi = \{\pi_i\}. \quad (3)$$

We model the signal received at the SU as a noisy version of the PU's actual signal, i.e.,

$$Y_t = S_t X_t + W_t, \quad (4)$$

where  $X_t$  is the PU signal, and  $W_t$  is modeled as additive white Gaussian noise (AWGN) with mean zero and variance  $\sigma_w^2$ . The SU cannot directly observe the states of the Markov process at the PU, rather its observations are probabilistic functions of the true state. This results in a hidden Markov model (HMM). A HMM consists of a non-observable (hidden) Markov chain  $\underline{S} = (S_1, S_2, \dots)$  and a measured output process  $\underline{Y} = (Y_1, Y_2, \dots)$  whose distribution is determined by  $\underline{S}$ . Note that we denote vectors by underlined variables throughout. In addition to  $P$  and  $\Pi$  needed to specify the hidden Markov chain, a HMM also requires emission probabilities, a set of functions of the form  $f_{Y_t | \underline{S}^t, \underline{Y}^{t-1}}(y_t | \underline{s}^t, \underline{y}^{t-1})$ , which is the probability density function (pdf) of the observed data  $y_t$  given the previous observation sequence  $\underline{y}^{t-1} = (y_1, y_2, \dots, y_{t-1})$  and state sequence  $\underline{s}^t = (s_1, s_2, \dots, s_t)$ . The goal of a spectrum sensing algorithm is to uncover the hidden channel states  $\underline{S}$  up to time  $T$ , i.e.,  $(S_1, S_2, \dots, S_T)$ , using the SU's observation sequence  $(Y_1, Y_2, \dots, Y_T)$ .

#### IV. WEIGHTED SEQUENCE DETECTION ALGORITHMS

In proposed DSA networks, the SU is generally under a strict requirement to limit interference to the PU as much as possible. Missed detections, therefore, may be more costly than false alarms, as they lead to collisions with the PU. We employ a Bayesian sequence detection framework that allows assignment of different costs for the two types of errors. This makes it possible to bias the detector in favor of reducing  $P_m$  at the expense of increasing  $P_f$  while still exploiting the Markov memory.

We start with a general formulation for the Bayesian sequence detector. For a length  $T$  binary sequence, there are  $2^T$  possible state sequences, which we denote  $\underline{s}^{(i)}$  for  $i \in \{1, \dots, 2^T\}$ . Let  $C_{ij} = C(\underline{s}^{(i)}, \underline{s}^{(j)})$  be the cost of declaring state sequence  $\underline{s}^{(i)}$  when the real state sequence is  $\underline{s}^{(j)}$ . Define the sequence risk function  $\mathcal{R}(\underline{s}^{(i)}|\underline{Y})$  as the expected value of the cost of declaring state sequence  $\hat{\underline{S}} = \underline{s}^{(i)}$  given the observation data sequence  $\underline{Y}$ , i.e.,

$$\begin{aligned} \mathcal{R}(\underline{s}^{(i)}|\underline{Y}) &= \mathbf{E}[C(\underline{s}^{(i)}, \underline{S})|\underline{Y}] \\ &= \sum_{j=1}^{2^T} C(\underline{s}^{(i)}, \underline{s}^{(j)})P(\underline{s}^{(j)}|\underline{Y}). \end{aligned} \quad (5)$$

Our objective is to find the state sequence that minimizes the associated sequence risk given the observation sequence  $\underline{Y} = \underline{y}$ , i.e.,

$$\hat{\underline{S}} = \arg \min_{\underline{s}^{(i)}, 1 \leq i \leq 2^T} \mathcal{R}(\underline{s}^{(i)}|\underline{Y} = \underline{y}). \quad (6)$$

Generally, the minimization is taken over a set with a total number of elements  $2^T$ , the computation time of which increases exponentially with the sequence length  $T$ . However, there are some special cases for which linear computation time algorithms exist.

##### A. Impulse Sequence Cost and the Viterbi Algorithm

If the sequence cost is an impulse function defined as

$$C_{ij} = \begin{cases} 0, & \text{if } \underline{s}^{(i)} = \underline{s}^{(j)} \\ 1, & \text{if } \underline{s}^{(i)} \neq \underline{s}^{(j)} \end{cases}, \quad (7)$$

i.e., all possible sequence errors are given the same weight, then the risk function becomes

$$\mathcal{R}(\underline{s}^{(i)}|\underline{Y}) = \sum_{j \neq i} P(\underline{s}^{(j)}|\underline{Y}) = 1 - P(\underline{s}^{(i)}|\underline{Y}). \quad (8)$$

Therefore, minimizing  $\mathcal{R}(\underline{s}^{(i)}|\underline{Y})$  is equivalent to maximizing  $P(\underline{s}^{(i)}|\underline{Y})$ , or choosing the state sequence that has the largest a posterior probability. We call it the sequence maximum a posterior (sequence-MAP) detector, which can be implemented using the well-known Viterbi algorithm [11], [12].

We apply the Viterbi algorithm with soft inputs to the spectrum sensing problem, which can be simplified to the hard input case at the expense of sensing performance. Throughout

this paper we make a fundamental assumption that the received samples in the observation sequence are conditionally independent given the state sequence, i.e.,

$$f_{Y_t|\underline{S}^t, \underline{Y}^{t-1}}(y_t|\underline{s}^t, \underline{y}^{t-1}) = f_{Y_t|S_t}(y_t|s_t), \quad (9)$$

where  $f_{Y_t|S_t}(y_t|s_t)$  is the probability density function of observing  $y_t$  given state  $s_t$ .

To briefly describe the Viterbi algorithm, let  $\delta_t(i)$  be the probability of the most probable path ending in state  $i$  at time  $t$  given the whole observation sequence  $\underline{Y} = (Y_1, Y_2, \dots, Y_T)$ , where  $T$  is the length of a sensing window, i.e.,

$$\delta_t(i) = \max_{s_1, \dots, s_{t-1}} P(S_1 = s_1, \dots, S_{t-1} = s_{t-1}, S_t = i|\underline{Y}). \quad (10)$$

We can calculate  $\delta_t(i)$  recursively according to

$$\delta_t(i) = \max_{j \in \{0,1\}} [\delta_{t-1}(j)p_{ji}]f_{Y_t|S_t}(y_t|i) \quad (11)$$

with initialization

$$\delta_1(i) = \pi_i f_{Y_1|S_1}(y_1|i). \quad (12)$$

To retrieve the state sequence, we need to keep track of the argument  $\psi_t(i)$  that maximizes (11) for each  $t$  and state  $i$ , i.e.,

$$\psi_t(i) = \arg \max_{j \in \{0,1\}} \delta_{t-1}(j)p_{ji}, \quad 2 \leq t \leq T. \quad (13)$$

At the end of the algorithm, the highest probability endpoint is chosen and the highest probability path (state sequence) is backtracked:

$$\hat{S}_T = \arg \max_{i \in \{0,1\}} \delta_T(i), \quad (14)$$

$$\hat{S}_t = \psi_{t+1}(\hat{S}_{t+1}), \quad t = T-1, T-2, \dots, 1. \quad (15)$$

In practice, the logarithmic version of the Viterbi Algorithm is often used due to its lower computational complexity and better numerical stability. The major drawback to using the Viterbi algorithm for spectrum sensing is it does not allow costs to be differentiated based on the types or numbers of errors. We have mentioned previously that missed detection errors may be much more costly to a spectrum sensing system than false alarms, which motivates development of other algorithms for such applications.

##### B. Additive Sequence Cost and the Forward-Backward Algorithm

Suppose the sequence cost is additive, i.e.,

$$C_{ij} = C(\underline{s}^{(i)}, \underline{s}^{(j)}) = \sum_{t=1}^T C(s_t^{(i)}, s_t^{(j)}), \quad (16)$$

where  $s_t^{(i)}$  is the state of the sequence  $\underline{s}^{(i)}$  at time  $t$  and  $C_{ij} = C(i, j)$  is the cost of declaring state  $i$  when the real state is  $j$  at any time instant. Define  $\mathcal{R}_t(i|\underline{Y})$  as the symbol risk function of declaring state  $i$  at time instant  $t$ ,  $1 \leq t \leq T$ , given the whole observation sequence  $\underline{Y} = (Y_1, Y_2, \dots, Y_T)$

$$\mathcal{R}_t(i|\underline{Y}) = \sum_{j \in \{0,1\}} C_{ij}P(S_t = j|\underline{Y}). \quad (17)$$

The sequence risk function can thus be written as a sum of the symbol risk functions:

$$\begin{aligned}
\mathcal{R}(\underline{s}^{(i)}|\underline{Y}) &= \mathbf{E}\left[\sum_{t=1}^T C(s_t^{(i)}, S_t)|\underline{Y}\right] \\
&= \sum_{t=1}^T \mathbf{E}[C(s_t^{(i)}, S_t)|\underline{Y}] \\
&= \sum_{t=1}^T \sum_{s_t \in \{0,1\}} C(s_t^{(i)}, s_t) P(S_t = s_t|\underline{Y}) \\
&= \sum_{t=1}^T \mathcal{R}_t(s_t^{(i)}|\underline{Y}), \tag{18}
\end{aligned}$$

where  $s_t^{(i)} \in \{0,1\}$ . This result demonstrates that if the sequence cost is additive, the sequence risk function is also additive under the reasonable assumption that all symbol risks are non-negative. Therefore, the state sequence can be estimated in a symbol-by-symbol fashion

$$\hat{S}_t = \arg \min_{i \in \{0,1\}} \{\mathcal{R}_t(i|\underline{Y} = \underline{y})\}. \tag{19}$$

The symbol a posteriori probability  $P(S_t = i|\underline{Y})$  in (17) can be calculated using the well-known forward-backward algorithm [12]. This algorithm has three steps:

- 1) Compute forward probabilities for each time instant,
- 2) Compute backward probabilities for each time instant,
- 3) Compute the a posteriori probability of each state for each time instant based upon the forward and backward probabilities.

These three steps are now summarized in more detail based upon [12].

1) *Forward Probabilities:* Let  $\alpha_t(i)$  be the joint probability density function of the partial observation sequence  $\underline{y}^t = (y_1, y_2, \dots, y_t)$  and state  $s_t = i$  at time  $t$ , i.e.,

$$\alpha_t(i) = f_{\underline{Y}^t, S_t}(y^t, i) \tag{20}$$

$\alpha_t(i)$  is proportional to the likelihood of the past observations and can be solved recursively according to

$$\alpha_1(i) = \pi_i f_{Y_1|S_1}(y_1|i) \tag{21}$$

$$\alpha_t(i) = \left( \sum_{j \in \{0,1\}} \alpha_{t-1}(j) p_{ji} \right) f_{Y_t|S_t}(y_t|i) \tag{22}$$

for  $2 \leq t \leq T$ . The recursive computation of the forward probabilities is illustrated in the trellis of Fig. 1.

2) *Backward Probabilities:* Let  $\beta_t(i)$  be the conditional probability of the partial observation sequence from  $y_{t+1}$  to the end produced by all state sequences that start at the  $i$ -th state

$$\beta_t(i) = f_{Y_{t+1}, \dots, Y_T|S_t}(y_{t+1}, \dots, y_T|i). \tag{23}$$

By definition,  $\beta_T(i) = 1$ .  $\beta_t(i)$  is proportional to the likelihood of the future observations and can be solved recursively according to

$$\beta_t(i) = \sum_{j \in \{0,1\}} p_{ij} f_{Y_{t+1}|S_{t+1}}(y_{t+1}|j) \beta_{t+1}(j) \tag{24}$$

for  $t = T-1, T-2, \dots, 1$ .

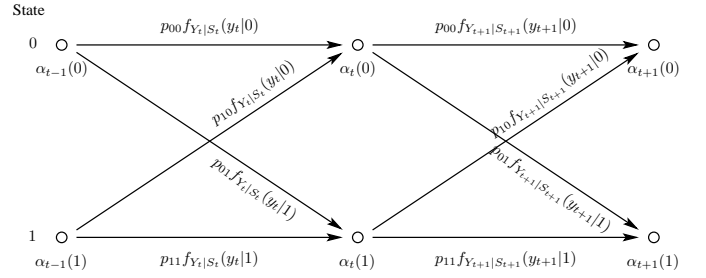


Fig. 1. Computing the forward probabilities.

3) *A Posteriori Probability of an Individual Symbol:* Let  $f_{\underline{Y}}(y)$  be the probability density function of observation  $\underline{Y}$ .  $f_{\underline{Y}}(y)$  can be calculated in three ways,

$$\begin{aligned}
f_{\underline{Y}}(y) &= \sum_{i \in \{0,1\}} \alpha_T(i) \\
&= \sum_{i \in \{0,1\}} \pi_i f_{Y_1|S_1}(y_1|i) \beta_1(i) \\
&= \sum_{i \in \{0,1\}} \alpha_t(i) \beta_t(i) \tag{25}
\end{aligned}$$

for any  $1 \leq t \leq T$ .

Let  $\lambda_t(i)$  be the a posteriori probability that the hidden state at time  $t$  is  $i$  for the given observation sequence  $\underline{Y} = \underline{y}$  up to time  $T$ ,

$$\lambda_t(i) = P(S_t = i|\underline{y}) = \frac{f_{\underline{Y}, S_t}(y, i)}{f_{\underline{Y}}(y)} = \frac{\alpha_t(i) \beta_t(i)}{f_{\underline{Y}}(y)}. \tag{26}$$

Then, the symbol-wise detection rule in (19) becomes

$$\hat{S}_t = \arg \min_{i \in \{0,1\}} \mathcal{R}_t(i|\underline{y}) = \arg \min_{i \in \{0,1\}} \sum_{j \in \{0,1\}} C_{ij} \lambda_t(i). \tag{27}$$

The above described algorithm is a weighted forward-backward algorithm. Note that the standard forward-backward algorithm without assigned costs (equivalent to uniform costs) chooses the state that maximizes the a posteriori probability of a symbol at each time instant [12],

$$\hat{S}_t = \arg \max_{i \in \{0,1\}} \lambda_t(i), \tag{28}$$

and is therefore a symbol-MAP detector that does not differentiate missed detections and false alarms. With costs assigned to the four different possibilities, our decision rule (19) for additive cost sequence detection corresponds to a more general form of the symbol-MAP detection rule. It is trivial to prove that if  $C_{00} = C_{11} = 0$  and  $C_{01} = C_{10} = 1$ , (19) reduces to (28).

It is also worth noting that provided a hardware realization for the symbol-MAP detection algorithm, it can be readily extended to the additive cost sequence detection algorithm by converting the symbol a posteriori probability for each state into the symbol risk for each state via (17).

Since  $C_{ij}$  is the cost of declaring state  $i$  when the real hidden state is  $j$ ,  $C_{01}$  and  $C_{10}$  are the costs for missed detection and false alarm, respectively. For DSA systems, it is natural to assign  $C_{00} = C_{11} = 0$  and  $C_{01}$  a higher cost than  $C_{10}$ , since missed detections may cause more harm than

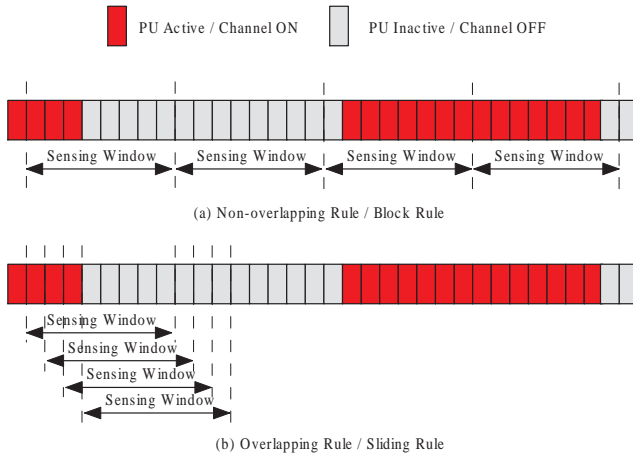


Fig. 2. Non-overlapping (block) rule and overlapping (sliding) rule.

false alarms. Essentially, it is the ratio between the costs of missed detection and false alarm that affects the operating point. Intuitively, the larger  $C_{01}$  is relative to  $C_{10}$ , the more the additive cost sequence detection algorithm is biased toward reducing  $P_m$  at the expense of increasing  $P_f$ . In the extreme case, if the cost for a missed detection is arbitrarily large, the algorithm will always declare the PU to be present, giving  $P_f = 1$  and  $P_m = 0$ . On the other hand, if the cost for a false alarm is arbitrarily large, the algorithm will always declare the spectrum to be available, giving  $P_f = 0$  and  $P_m = 1$ . By varying the relative costs, we obtain different operating pairs of  $(P_f, P_m)$  corresponding to different points on the receiver operating characteristic (ROC) curve for the sequence detector.

### C. Overlapping and Non-Overlapping Sensing Rules

For each spectrum sensing algorithm there are at least two ways of using the observed data and making decisions. One method is to make decisions on a block-by-block basis, corresponding to using each observation in only one sensing window. The SU collects a window of data, processes the data, makes decisions for the current window, and then discards the data (vacate the buffer) to start the sensing procedure for the next sensing window. We call this a non-overlapping (block) detection rule. The other method is to make a decision at each time instant using a sliding window, adding new observations one at a time and dropping the oldest observation. Note that a single observation factors into multiple windows and thus multiple decisions. We call this an overlapping (sliding) detection rule. Also note that for non-overlapping energy detection and coherent detection, the detector makes a single decision for each block, assuming all the symbols in the sensing window have the same state. These two procedures are illustrated in Fig. 2. Intuitively, employing an overlapping rule subjects the SU to less sensing delay since decisions are made right after an observation. For a non-overlapping rule, the sensing delay is on the order of sensing window length.

In the worst case, the average computation time for a sliding rule can be  $T$  times as large as that of a block rule. However, more efficient algorithms exist for both energy detection and weighted sequence detection. For energy detection, we can

use a moving average to eliminate reduplicate computations. For our sliding weighted sequence detection algorithm, we are really only interested in the decision at the current time instant. Thus it may not be necessary to calculate any backward probabilities and only the forward probabilities for the states at the most recent time instant is needed to be stored due to the recursive nature of their calculation. We refer to this simplification as the *complete forward algorithm (CFA)*. In essence, CFA's memory can be infinitely long.

Although CFA has infinite memory length and can make decisions instantaneously, it does not fully exploit the memory inherent in the underlying Markov process and its performance may be worse than the weighted forward-backward algorithm. We can, however, increase performance by propagating backward a few symbols to better exploit the memory in the data at the cost of increased sensing delay. We call this algorithm the *complete forward partial backward algorithm (CFPB)*. Clearly the performance of CFPB lies somewhere between that of CFA and the weighted forward-backward algorithm with an infinitely long sensing window, giving a tradeoff between sensing performance and sensing delay/complexity.

### V. COMPARISON TO ENERGY AND COHERENT DETECTION

In this section, we introduce a new limitation of standard energy and coherent detection. The first part of this section is not really something new, but we review energy detection and coherent detection and discuss their threshold selection to the problem of minimizing the detection risk given the cost factors. This is done by relating their thresholds to that of the proposed weighted forward-backward algorithm in an extreme case. In the second part, we then introduce the new fundamental limitation which we call the *risk floor*.

We start our discussion from the extreme case in which there is no state change within one sensing window. This condition corresponds to a scenario in which the transition probabilities  $p_{01} = p_{10} = 0$ . In this case, the proposed weighted forward-backward sequence detection algorithm can be reduced to

$$\frac{f_{Y|S}(y|0)}{f_{Y|S}(y|1)} \underset{1}{\overset{0}{\gtrless}} \epsilon_s, \quad (29)$$

where  $\epsilon_s = [\pi_1(C_{01} - C_{11})]/[\pi_0(C_{10} - C_{00})]$ . The result corresponds to the classical likelihood ratio test for minimizing the risk function [13]. Let  $\mathbb{A}$  be the ON-decision region for a detector. We use the term ‘‘decision region’’ exclusively for the case in which there is no state change in a sensing window for the weighted forward-backward algorithm, since only in this case will the detector make the same decision for every symbol in the block, i.e., it is a block decision rather than a sequence of individual decisions. For energy detection and coherent detection which make a single decision for each block, the term ‘‘decision region’’ always makes sense. The ON-decision region  $\mathbb{A}_S$  for the weighted sequence detection algorithm is obvious from Eq. (29).

#### A. Threshold for Energy Detection and Coherent Detection

If the signal and the noise process both follow zero-mean identical independent Gaussian distributions, weighted

forward-backward algorithm is equivalent to energy detection for the extreme case in which it is guaranteed no state change occurs in a sensing window. To see this, let  $\epsilon_s$  be the threshold for the weighted sequence detection and  $\epsilon_e$  be the threshold for energy detection.  $\epsilon_s$  and  $\epsilon_e$  are chosen such that they give the same false alarm probabilities  $\bar{P}_f$ . The ON-decision region for energy detection is [1]

$$\mathbb{A}_E = \left\{ \underline{y} \left| \frac{1}{T} \sum_{t=1}^T |y_t|^2 > \epsilon_e(\bar{P}_f) \right. \right\}. \quad (30)$$

On the other hand, the ON-decision region for the weighted forward-backward algorithm can be simplified to

$$\mathbb{A}_S = \left\{ \underline{y} \left| \frac{1}{T} \sum_{t=1}^T |y_t|^2 > \frac{2\sigma_0^2\sigma_1^2}{\sigma_1^2 - \sigma_0^2} \left( \ln \frac{\sigma_1}{\sigma_0} - \frac{1}{T} \ln \epsilon_s(\bar{P}_f) \right) \right. \right\}, \quad (31)$$

where  $\sigma_0^2 = \sigma_w^2$  and  $\sigma_1^2 = \sigma_w^2 + \sigma_x^2$ . Since the ON-decision region for sequence detection and energy detection are both  $T$ -dimensional balls, one should be a subset of the other in the  $T$ -dimensional space, and for the same false alarm probabilities, they should be identical, which in turn gives

$$\epsilon_e(\bar{P}_f) = \frac{2\sigma_0^2\sigma_1^2}{\sigma_1^2 - \sigma_0^2} \left( \ln \frac{\sigma_1}{\sigma_0} - \frac{1}{T} \ln \epsilon_s(\bar{P}_f) \right). \quad (32)$$

Therefore, the detection probabilities are the same as well.

Although (30), (31) and (32) show the decision regions for energy detection and weighted forward-backward algorithm are the same under the concerned condition, the importance of these equations goes beyond this. Since  $\epsilon_s = [\pi_1(C_{01} - C_{11})]/[\pi_0(C_{10} - C_{00})]$ , Eq. (32) essentially relates the threshold for energy detection to the cost factors for missed detections and false alarms and results in an optimal threshold in the sense of minimizing the detection risk. Compared to the often-used Gaussian approximation according to central limit theorem for  $\sum_{t=1}^T |y_t|^2/T$  [1], here we provide an accurate computation for the optimal threshold for energy detection that minimizes the expected cost. As standard energy detection does not consider the PU's channel access pattern, it always uses the threshold derived above to minimize the detection risk given the cost factors.

It is also worth noting that the proposed sequence detection algorithms we derived in Section IV depend on accurate knowledge of the distribution of the observed symbols given the channel state as well as the channel state transition probabilities. However, for one thing, these parameters can be estimated by the Baum-Welch algorithm [12], which we will study in our future work. For another, if the conditional pdf cannot be obtained anyway, we can integrate energy detection and the sequence detection algorithms by dividing the whole sensing window into a sequence of sub-windows and applying energy detection and Gaussian approximation according to central limit theorem to each sub-window. In this way, we cannot only implement the proposed sequence detection algorithms with insufficient statistics, but also reduce the computational complexity. The expense of this integration of energy detection and sequence detection algorithms is an increasing granularity and possible sensing delay.

Another scenario can arise if the PUs spare a certain amount of energy to transmit pilot signals. For simplicity, we assume the PU always transmits 1 with normalized signal power when it is occupying the channel. In this case, the threshold for coherent detection  $\epsilon_c$  can be related to that of the sequence detection by

$$\epsilon_c(\bar{P}_f) = \frac{1}{2} + \frac{\sigma_w^2}{T} \ln \epsilon_s(\bar{P}_f). \quad (33)$$

### B. Risk Floor For Energy Detection

For the weighted forward-backward algorithm that minimizes the detection risk, we expect the risk to decrease continuously with increasing SNR. However, for energy detection, there exists a certain risk level that it cannot surpass even with an arbitrarily large SNR. We call this limit the *risk floor*. The *risk floor* is caused by finite PU dwell time. We will provide an approximation for the risk floor in this section and validate its existence in the next section.

We start with a theorem that essentially states that even one ON symbol in a sensing window can trigger the energy detector to make an ON decision with high probability if the SNR is large.

*Theorem:* Suppose the PU follows a certain spectrum access pattern and its dwell time is finite. If the optimal threshold  $\epsilon_e$  in (32) that minimizes the detection risk for the given four cost factors is applied for energy detection, then

$$P\left(\frac{1}{T}|X_\tau + W_\tau|^2 > \epsilon_e\right) \rightarrow 1, \quad \text{as SNR} \rightarrow \infty, \quad (34)$$

where  $\tau$  is any time instant within a sensing window.

*Proof:* Without loss of generality, let  $\sigma_0^2 = \sigma_w^2 = 1$ . Define  $\text{SNR} = 10 \log_{10}(\sigma_x^2/\sigma_n^2) = 20 \log_{10} \sigma_x$ . For high SNR,

$$\begin{aligned} \epsilon_e &= 2 \left( \ln \sigma_x - \frac{1}{T} \ln \frac{\pi_1(C_{01} - C_{11})}{\pi_0(C_{10} - C_{01})} \right) \\ &= \frac{\ln 10}{10} \text{SNR} - \frac{2\epsilon_s}{T}. \end{aligned} \quad (35)$$

Therefore,

$$\begin{aligned} P\left(\frac{1}{T}|X_\tau + W_\tau|^2 > \epsilon_e\right) &\approx P\left(\frac{1}{T}|X_\tau|^2 > \epsilon_e\right) \\ &= 2P(X_\tau > \sqrt{\epsilon_e T}) \\ &= 2Q\left(\sqrt{\frac{\frac{\ln 10}{10} T \cdot \text{SNR} - 2\epsilon_s}{10 \frac{\text{SNR}}{10}}}\right) \\ &\rightarrow 1 \end{aligned} \quad (36)$$

as  $\text{SNR} \rightarrow \infty$  for fixed  $T$  and  $\epsilon_s$ . Furthermore,

$$P\left(\frac{1}{T} \sum_{t=1}^T |Y_t|^2 > \epsilon_e\right) > P\left(\frac{1}{T}|X_\tau + W_\tau|^2 > \epsilon_e\right) \rightarrow 1 \quad (37)$$

as  $\text{SNR} \rightarrow \infty$  as well if  $Y_\tau = X_\tau + W_\tau$  is an ON symbol. ■

This theorem implies that for high SNR, a sensing window with even one ON symbol will lead to an ON decision. Obviously, the probability of missed detection goes to zero and the risk is dominated by false alarm, which can be either of the two types illustrated in Fig. 3. Note that type II may not be called a false alarm since it makes a correct decision

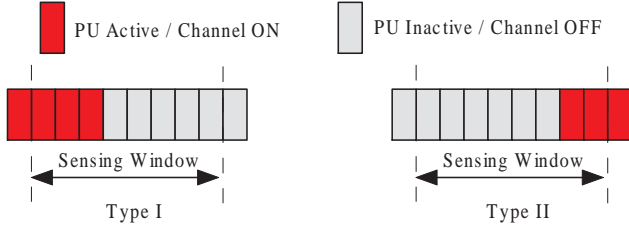


Fig. 3. Two scenarios leading to false alarms for energy detection when the PU state changes during a sensing window.

for the channel's future state by declaring the channel is ON. However, for simplicity, we assume the SU continuously senses the spectrum without transmitting and the decision is made for the current block or symbol. Therefore, the ON decision for the whole block leads to false alarms for the first part of the sensing window in which the channel is still OFF as shown in the figure.

We will only consider the case in which the window length  $T \ll \min\{\mathbf{E}[L_0], \mathbf{E}[L_1]\}$  since things get even worse when  $T$  is comparable to  $\mathbf{E}[L_0]$  and  $\mathbf{E}[L_1]$  as we will see in the numerical results. Type I corresponds to the case in which the channel changes from state ON to OFF in a sensing window. The condition  $T \ll \min\{\mathbf{E}[L_0], \mathbf{E}[L_1]\}$  guarantees that the probability of multiple channel state changes during one sensing window is negligible in computing the channel state change probability in a sensing window. The symbol risk for type I false alarm is

$$\begin{aligned} \mathcal{R}_I &= \pi_1 C_{01} \prod_{t=1}^{T-1} \left( P(L_1 = t) \cdot \frac{T-t}{T} \right) \\ &= \pi_1 C_{01} \left( 1 - \frac{1-p_{11}^T}{T p_{10}} \right). \end{aligned} \quad (38)$$

Similarly, the symbol risk for type II false alarm is

$$\begin{aligned} \mathcal{R}_{II} &= \pi_0 C_{10} \prod_{t=1}^{T-1} \left( P(L_0 = t) \cdot \frac{t}{T} \right) \\ &= \pi_0 C_{10} \left( \frac{1-p_{00}^T}{T p_{01}} - p_{00}^{T-1} \right). \end{aligned} \quad (39)$$

Thus, we approximate the risk floor of energy detection by

$$\mathcal{R}_F \approx \mathcal{R}_I + \mathcal{R}_{II}. \quad (40)$$

Intuitively, false alarms are caused primarily by randomness and confusion in the primary signal and noise for low SNR, and they are dominated by channel state changes for high SNR. Since the risk floor results from not considering channel state changes, it can be shown in a similar way that the risk floor arises for coherent detection as well. Numerical results verifying the existence of this risk floor are provided in the following section.

## VI. NUMERICAL RESULTS

This section provides numerical results demonstrating the improved performance that the developed sequence detection algorithms exhibit over energy and coherent detection. For simplicity, we assume the SU continuously senses the spectrum and never transmits.

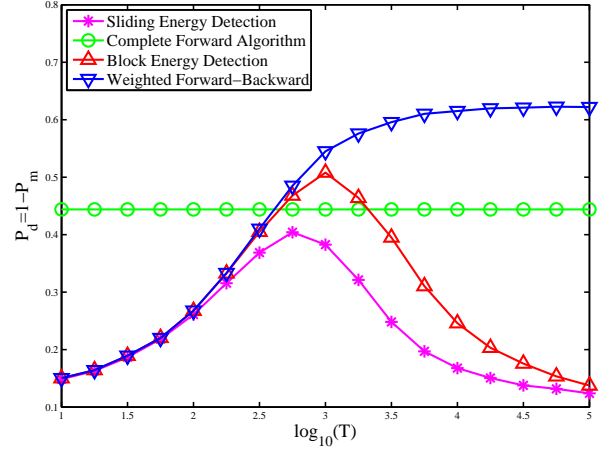


Fig. 4. Detection performance and sensing window length.  $\mathbf{E}[L_0] = 2000$ ,  $\mathbf{E}[L_1] = 1000$ , SNR=-10dB,  $\bar{P}_f = 0.1$ .

### A. Sequence Detection versus Energy and Coherent Detection

We first consider a specific realization in which some proposed sequence detection algorithms and energy detection are applied. Let  $\mathbf{E}[L_0] = 2000$  and  $\mathbf{E}[L_1] = 1000$ , which give state transition probabilities  $p_{01} = 0.0005$  and  $p_{10} = 0.001$ . The signal and noise variance are set so that SNR = -10 dB. In Fig. 4, we plot the detection probability versus sensing window length  $T$  for a fixed false alarm probability  $\bar{P}_f = 0.1$ . The result for CFA is independent of  $T$  and is provided for comparison. The simulation leads to several important conclusions.

First, if  $T \ll \min\{\mathbf{E}[L_0], \mathbf{E}[L_1]\}$ , which implies that the probability of channel state change within a sensing window is relatively small, the performance of the weighted sequence detection algorithm, non-overlapping energy detection and overlapping energy detection are very similar. However, if the length of the sensing window is comparable to the average length of an ON/OFF period, the effect of state changes in a sensing window comes into play and the performance of energy detection is seriously affected since it does not take into account the PU dwell time. On the other hand, the performance of the weighted sequence detection algorithm continues to improve with increasing window length. The performance does not degrade since the algorithm itself takes possible state change into consideration.

Second, for both overlapping and non-overlapping energy detection, there is an optimal window length  $T^*$  that gives the best detection probability  $P_d^*$  for a fixed  $\bar{P}_f$ , given SNR and the PU's channel access statistics. If the window length exceeds  $T^*$ , the detection performance degrades because the energy detector groups observations from multiple PU states. Although no theoretical analysis is provided here, we call this limitation of energy detection (and coherent detection in the next example) the *window length limitation*. It is another limitation for spectrum sensing performance besides the well-known SNR-wall [2]. Moreover, the proposed sequence detection algorithms cannot achieve arbitrary large detection probability even with infinite window length. On the contrary,

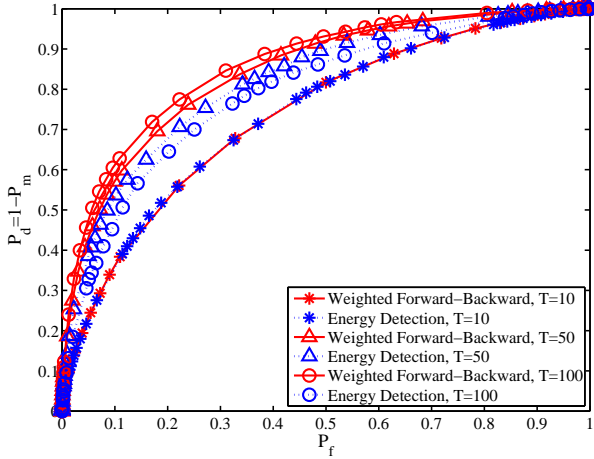


Fig. 5. Receiving Operating Characteristics.  $\mathbf{E}[L_0] = 100$ ,  $\mathbf{E}[L_1] = 50$ ,  $\text{SNR} = -10\text{dB}$ .

the detection probability corresponding to a given false alarm probability approaches a limit as  $T$  becomes large as shown in the figure. This implies that PHY-layer detection algorithms are performance limited by the PU's channel access pattern. Nevertheless, our proposed sequence detection algorithms outperform the standard energy detection in a number of ways. We also notice an advantage of the non-overlapping rule over the overlapping rule with regards to operating pairs.

Now we consider an example of coherent detection. If the primary signal is known to the secondary user and coherent detection is used, the sensing window can be much shorter than that of energy detection to achieve the same operating pair. Therefore, in order to clearly see the advantage of sequence detection over coherent detection, we consider a smaller sensing window length and PU dwell time. The expected OFF and ON dwell times are  $\mathbf{E}[L_0] = 100$  and  $\mathbf{E}[L_1] = 50$ , and SNR is  $-10$  dB again. We compare the performance by plotting the ROC curves for three window lengths as shown in Fig. 5. As the results show, weighted forward-backward and coherent detection have similar ROC curves when  $T$  is relatively small. As  $T$  increases, the ROC curves of coherent detection begin to fall below that of the weighted forward-backward. The ROC curves for coherent detection even begin to degrade after a certain  $T$ , while on the other hand, the ROC curves of sequence detection continues to improve with increasing  $T$ . However, the curves converge as  $T$  goes to infinity. These results agree with the conclusions made from Fig. 4.

### B. CFA versus CFPB

We now compare the sensing performance of CFA and CFPB with different backward window lengths  $l_B$  by plotting risk as a function of SNR. As the simulation results in Fig. 6 show, even use of one symbol of backward processing increases the sensing performance significantly and this gain increases with SNR. Another interesting fact is that for high SNR, the performance of CFPB quickly approaches a limit and increasing  $l_B$  beyond a certain number barely improves the sensing performance. For the simulation environment in Fig. 6,

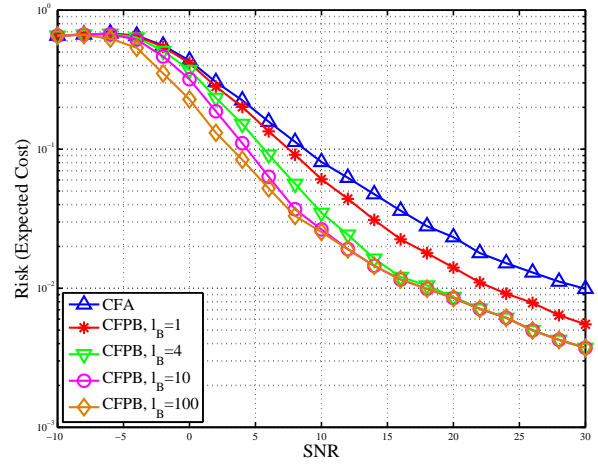


Fig. 6. Risk performance for CFA and CFPB.  $\mathbf{E}[L_0] = 200$ ,  $\mathbf{E}[L_1] = 100$ ,  $C_{01} = 10C_{10}$ .

CFPB with a backward window length of 4 symbols performs almost as well as CFPB with backward window length of 100 symbols, although large backward window length offers more advantage for moderate SNR ( $-5\text{dB}$  to  $10\text{dB}$  in Fig. 6).

For high SNR, in which case the CFPB converges for increasing backward window length, we observe a gain of about 10 dB for CFPB over CFA.

### C. Risk Floor for Energy Detection

We compare the performance of energy detection, sequence-MAP and symbol-MAP with weighted forward-backward algorithm for  $T \ll \min\{\mathbf{E}[L_0], \mathbf{E}[L_1]\}$  and the cost for missed detections much higher than the cost for false alarms, for two scenarios differing in sensing window length. Fig. 7 and Fig. 8 both show that the performance of sequence-MAP and symbol-MAP are surprisingly similar, which makes sense intuitively since, making the sequence error small will also make the symbol error small. Moreover, the weighted forward-backward algorithm significantly outperforms sequence-MAP and symbol-MAP which do not differentiate missed detections and false alarms. We observe a gain analogous to that of ‘‘coding gain’’ for the weighted forward-backward algorithm, which is about 1 dB when the risk is  $10^{-2}$  and 6 dB when the risk is  $10^{-3}$  for  $T = 10$ , and 2 dB when the risk is  $10^{-2}$  and about 10 dB when the risk is  $10^{-3}$  for  $T = 100$ . We also observe that the performance of sequence-MAP and symbol-MAP are extremely bad at low SNR, even worse than that of energy detection.

Another important observation from these simulation results is the validation of the existence of the risk floor for energy detection. We notice that the risks for the weighted forward-backward algorithm decrease with asymptotically fixed slopes as SNR increases, however, for energy detection the risk approaches the risk floor and cannot be decreased, regardless of the window length. The risk floor shown in the simulation results also validates the theoretical analysis in (40). For  $T = 10$ ,  $\mathcal{R}_F = 0.003$  by Eq. (40), and the simulation result in

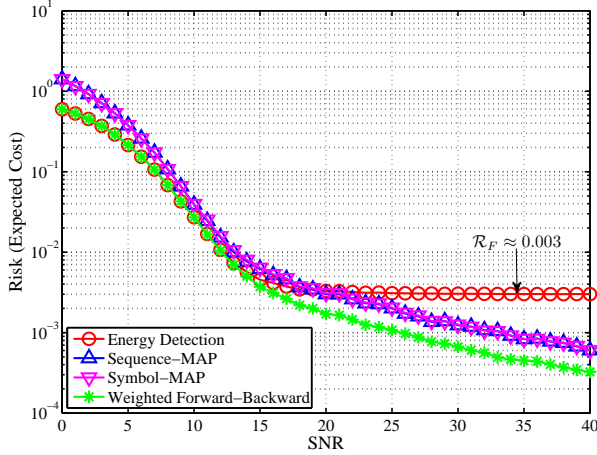


Fig. 7. The risk floor for energy detection.  $\mathbf{E}[L_0] = 2000$ ,  $\mathbf{E}[L_1] = 1000$ ,  $T = 10$ ,  $C_{01} = 10C_{10}$ .

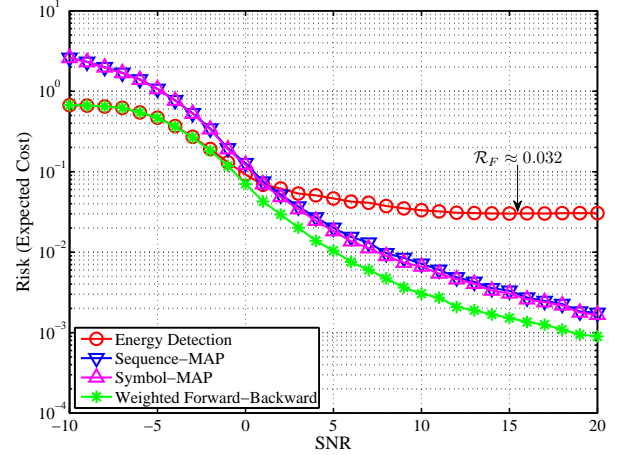


Fig. 8. The risk floor for energy detection.  $\mathbf{E}[L_0] = 2000$ ,  $\mathbf{E}[L_1] = 1000$ ,  $T = 100$ ,  $C_{01} = 10C_{10}$ .

Fig. 7 gives  $\mathcal{R}_F = 0.003$  as well. For  $T = 100$ ,  $\mathcal{R}_F = 0.032$  by Eq. (40), which is very close to  $\mathcal{R}_F = 0.031$  given by simulation results in Fig. 8. Therefore, (40) appears to be a good theoretical approximation for computing the risk floor of energy detection.

## VII. CONCLUSION

In this paper, we model the PU's access pattern by a Markov chain model and apply sequence detection algorithms for spectrum sensing in DSA networks. Specifically, we focus on the weighted soft-input sequence detection algorithm based upon forward-backward algorithm with additive, non-uniform costs. Besides the weighted forward-backward algorithm, the basic weighted sequence detection algorithm that derived directly from the forward-backward algorithm with cost factors assigned to false alarms and missed detections, we propose two types of advanced weighted sequence detection algorithms, which we call *complete forward algorithm (CFA)* and *complete forward partial backward (CFPB)*, and we show that they offer appealing tradeoffs between operating pair  $(P_f, P_m)$  and the sensing delay and complexity. We showed that the weighted forward-backward algorithm is optimal in minimizing the risk, i.e., the expected cost, and unlike energy detection, is robust to channel state changes in a sensing window. We compare by simulation the performance of the sequence detection algorithms with energy detection and coherent detection for the general case in which channel state is subject to changes in a sensing window. The results not only show that exploiting the memory of PU activity can improve the sensing performance, but also suggest new limitations for energy detection and coherent detection caused by finite PU dwell time, since longer observation windows are more likely to mix the PU's behavior from multiple states, leading to degraded performance. We call these limitations the *window length limitation* and the *risk floor*. Specifically, the window length limitation is most pronounced for low SNR, while the risk floor is typical for high SNR. We also generate a good approximation for computing the risk floor in this paper.

## ACKNOWLEDGEMENT

This work has been supported in part by NSF Grant CNS06-201072-31025 and NIJ Grant 2006-201075-31025.

## REFERENCES

- [1] D. Cabric, A. Tkachenko, and R. W. Brodersen, "Spectrum Sensing Measurements of Pilot, Energy and Collaborative Detection," *Proc. of IEEE Military Communications Conference*, Oct. 2006.
- [2] A. Sahai, N. Hoven, R. Tandra, "Some Fundamental Limits on Cognitive Radio," *Proc. of Allerton Conference*, Monticello, Oct 2004.
- [3] C. Ghosh, C. Cordeiro, D. P. Agrawal, and M. B. Rao, "Markov Chain Existence and Hidden Markov Models in Spectrum Sensing," *IEEE PerCom 2009*, pp. 1 - 6, Mar. 2009
- [4] H. Kim and K. G. Shin, "Efficient Discovery of Spectrum Opportunities with MAC-Layer Sensing in Cognitive Radio Networks," *IEEE Transactions on Mobile Computing*, Vol. 7, No. 5, pp 533-545, May 2008
- [5] D. Cabric, S. M. Mishra, and R. W. Brodersen, "Implementation Issues in Spectrum Sensing for Cognitive Radios," *Proc. Asilomar Conf. Signals, Systems, and Computers*, pp. 772-776, Nov. 2004.
- [6] Y. C. Liang, Y. Zeng, E. Peh, and A. Hoang, "Sensing-throughput tradeoff for cognitive radio networks," *IEEE Trans. Wireless Commun.*, Vol. 7, No. 4, pp. 1326-1337, Apr. 2008.
- [7] N. B. Chang, and M. Liu, "Optimal Channel Probing and Transmission Scheduling for Opportunistic Spectrum Access," *IEEE/ACM Transactions on Networking*, Vol. 17, No. 6, Dec 2009.
- [8] X. Y. Wang, A. Wong, and P. Ho, "Extended Knowledge-Based Reasoning Approach to Spectrum Sensing for Cognitive Radio," *IEEE Transactions on Mobile Computing*, Vol. 9, 2010.
- [9] S. Huang, X. Liu, and Z. Ding, "Optimal Sensing-Transmission Structure for Dynamic Spectrum Access," *IEEE InfoCom 2009*.
- [10] Q. Zhao, L. Tong, and A. Swami, "Decentralized Cognitive MAC for Dynamic Spectrum Access," *Proc. IEEE Int'l Symp. Dynamic Spectrum Access Networks (DySPAN '05)*, pp. 224-232, Nov. 2005.
- [11] G. D. Forney, "The Viterbi algorithm," *Proceedings of the IEEE*, Vol. 61, pp. 268-278, Mar. 1973.
- [12] L. R. Rabiner, "A Tutorial on Hidden Markov Models and Selected Applications in Speech Recognition," *Proceedings of the IEEE*, Vol. 77, pp. 257 - 286, Feb. 1989.
- [13] H. L. Van Trees, *Detection, Estimation, and Modulation Theory part I*, J. Wiley & Sons Inc., 1968.
- [14] G. D. Brushe, R. E. Mahony, and J. B. Moore, "A Soft Output Hybrid Algorithm for ML/MAP Sequence Estimation," *IEEE Transactions on Information Theory*, Vol. 44, No. 7, Nov 1998.
- [15] I. Akyildiz, W. Lee, M. Vuran, and S. Mohanty, "Next Generation/ Dynamic Spectrum Access/Cognitive Radio Wireless Networks: A Survey," *Elsevier Computer Networks*, Vol. 50, 2006, pp. 2127-2159.
- [16] Q. Zhao, and B. M. Sadler, "A Survey of Dynamic Spectrum Access: Signal Processing, Networking, and Regulatory Policy," *IEEE Sig. Processing*, May 2007.